ORIGINAL PAPER

Impact of right ventricular endocardial trabeculae on volumes and function assessed by CMR in patients with tetralogy of Fallot

Hendrik G. Freling · Kees van Wijk · Karolien Jaspers ·
Petronella G. Pieper · Karin M. Vermeulen ·
Jeroen M. van Swieten · Tineke P. Willems

Abstract The objective of this study was to assess the impact of right ventricular (RV) trabeculae and papillary muscles on measured volumes and function assessed by cardiovascular magnetic resonance imaging in patients with repaired tetralogy of Fallot. Sixty-five patients with repaired tetralogy of Fallot underwent routine cardiovascular magnetic resonance imaging. Endocardial and epicardial contours were drawn manually and included trabeculae and papillary muscles in the blood volume. Semi-automatic threshold-based segmentation software excluded these structures. Both methods were compared in terms of end-diastolic, end-systolic and stroke volume, ejection fraction and mass. Observer agreement was determined for all measures. Exclusion of trabeculae and papillary muscle in the RV blood volume decreased measured RV end-diastolic volume by 15 % (from 140 ± 35 to 120 ± 32 ml/m^2) compared to inclusion, end-systolic volume by 21 % (from 74 ± 23 to 59 ± 20 ml/m^2), stroke volume by 9 % (from 66 ± 16 to 60 ± 16 ml/m^2) and relatively increased ejection fraction by 7 % (from 48 ± 7 to 51 ± 8 %) and end-diastolic mass by 79 % (from 28 ± 7 to 51 ± 10 g/m^2), $p < .01$. Excluding trabeculae and papillary muscle resulted in an improved interobserver agreement of RV mass compared to including these structures (coefficient of agreement of 87 versus 78 %, $p < .01$). Trabeculae and papillary muscle significantly affect measured RV volumes, function and mass. Semi-automatic threshold-based segmentation software can reliably exclude trabeculae and papillary muscles from the RV blood volume.

Keywords Tetralogy of Fallot · Cardiovascular magnetic resonance imaging · Right ventricle · Trabeculae · Segmentation software

H. G. Freling · K. Jaspers · J. M. van Swieten ·
T. P. Willems (✉)
Department of Radiology, University Medical Center Groningen, University of Groningen, PO Box 30.001, 9700 RB Groningen, The Netherlands
e-mail: t.p.willems@umcg.nl

K. van Wijk
Medis Medical Imaging Systems BV, PO Box 384, 2300 AJ Leiden, The Netherlands

P. G. Pieper
Department of Cardiology, University Medical Center Groningen, University of Groningen, PO Box 30.001, 9700 RB Groningen, The Netherlands

K. M. Vermeulen
Epidemiology Unit HTA, University Medical Center Groningen, University of Groningen, PO Box 30.001, 9700 RB Groningen, The Netherlands

Introduction

Tetralogy of Fallot (ToF) is the most common congenital heart disease involving the right ventricle (RV). Important complications during follow-up after repair for ToF are RV volume overload. Longstanding volume overload can result in irreversible RV dilation and dysfunction which can be prevented by timely replacing the pulmonary valve [1–5]. Furthermore, many patients have some amount of pressure overload caused by residual outflow tract obstruction, stenosis of a pulmonary artery branch or stenosis of a valve prosthesis. Therefore, evaluation of the RV is essential in the follow-up of patients with ToF [6, 7].

Guidelines advise cardiac magnetic resonance imaging (CMR) as the primary imaging modality for evaluation of RV volumes and function [6, 7]. Consensus is lacking on whether to consider trabeculae and papillary muscles as

part of measured RV volumes [8–10]. Including trabeculae and papillary muscles in RV volumes results in larger measured volumes compared to measurements with exclusion of these structures. In healthy subjects and patients without congenital heart disease, the influence of trabeculae and papillary muscle on RV volumes is too small to be of clinical importance [9]. The increase in papillary muscle and trabeculae can be large in patients with a systemic right ventricle [10]. However, no studies have addressed the influence of papillary muscle and trabeculae on measured RV volumes in patients with repaired ToF. Studies in patients with ToF including trabeculae and papillary muscles in the RV blood volume report larger RV volumes and lower RV mass than studies excluding these structures [11–14]. Therefore, knowledge of the quantity of trabeculae and papillary muscles and the possibility to estimate this amount could be of clinical importance in patients with ToF.

The primary objective of our study was to determine the trabecular volume of the RV and the reliability by which it can be measured in patients with repaired ToF. The second objective was to create a mathematical model that describes the relation between the RV volumes with and without inclusion of trabeculae and papillary muscle in the RV blood volume.

Materials and methods

Patients

The study population consisted of 65 patients with repaired ToF. All patients underwent CMR examination between January 2008 and January 2011. In 60 (92 %) patients primary indication for CMR was follow-up of RV volumes and pulmonary flow parameters, in 3 (5 %) patients sudden decrease in exercise capacity, in 1 (2 %) patient new onset of ventricular tachycardia and in 1 (2 %) patient poor echocardiographic image quality. In 24 (37 %) patients clinical symptoms were present: subjective reduced exercise capacity in 14 (22 %) patients, history of supraventricular tachycardia in 5 (8 %) patients and history of ventricular tachycardia in 5 (8 %) patients. Other patient characteristics are shown in Table 1.

This retrospective study was approved by the University Medical Center Groningen review board and informed consent was not required according to the Dutch Medical Research Involving Human Subjects act.

CMR image acquisition

All subjects were examined on a 1.5-Tesla MRI system (Siemens Magnetom Sonata, Erlangen, Germany or

Table 1 Patient characteristics

Characteristic	
Male	37 (57)
Age (years)	30 ± 10
Body surface area (m^2)	1.86 ± 0.19
Age at total repair (years)	1.76 (0.89–5.05)
Pulmonary valve replacement	15 (23)
Pulmonary regurgitation fraction (%)	34 (15–45)
Pulmonary regurgitation volume (ml/m^2)	18 (7–30)
Pulmonary valve peak flow velocity (cm/s)	187 ± 75

Data are mean ± SD, median (IQR), or number of subjects (%)

Siemens Magnetom Avanto, Erlangen, Germany) using a 2 × 6 channel body-coil. After single-shot localizer images, short axis cine loop images with breath holding in expiration were acquired using a retrospectively gated balanced steady state free precession sequence. Parallel imaging was employed using GRAPPA (GeneRalized Autocalibrating Partially Parallel Acquisition). To improve image intensity uniformity Prescan Normalize was used. Short axis slices were planned in end-diastole from two slices above the mitral valve plane to the apex. The following parameters were used: TR 2.7 ms, TE 1.1 ms, flip angle 80°, matrix 192 mm × 192 mm, 25 frames per cycle, slice thickness 6 mm, interslice gap 4 mm, voxel size 1.7 mm × 1.7 mm × 6 mm.

Two-dimensional velocity encoded MRI flow measurements perpendicular and directly cranial to the pulmonary valve was performed to quantify flow velocity and volumes. Encoded velocity was 200 cm/s which was increased in steps of 50 cm/s in case of aliasing.

CMR image analysis

Image analysis was performed manually by using QMass MR (version 7.2, Medis, Leiden, The Netherlands) and semi-automatically by using QMass MR research edition (Medis, Leiden, The Netherlands).

The end-systolic and end-diastolic frames of the RV were selected by visual assessment. The basal slice was selected with aid of long-axis cine view images. When the pulmonary valve was visible in the RV basal slice, only the portion of the right ventricular outflow tract below the level of the pulmonary valve was included. The inflow part of the RV was included in the RV volume. The RV inflow part was distinguished from the right atrium by recognizing the trabeculated and thick right ventricular wall compared to the thin right atrial wall [15]. RV contours were drawn manually by tracing the endocardial and epicardial borders in every slice in end-systole and end-diastole. Contour tracing was aided by reviewing the multiple phase scans in the movie mode.
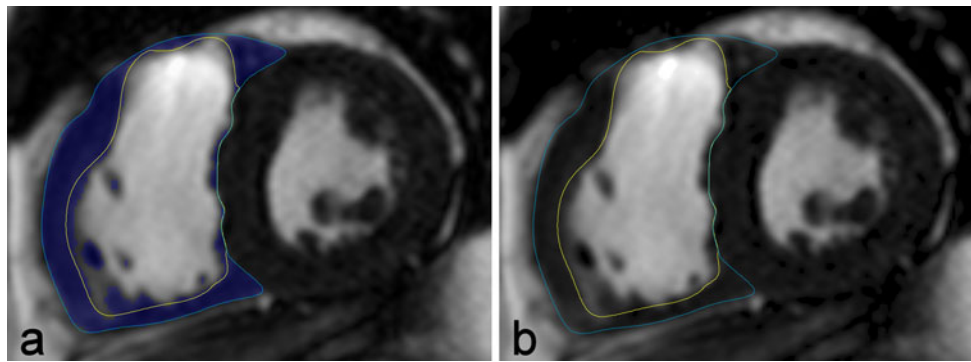
Fig. 1 Two methods were used to measure RV volumes. In method 1, trabeculae and papillary muscle were excluded from the right ventricular volume with use of semi-automatic threshold-based segmentation software (**a**). In method 2, trabeculae and papillary muscle were included in the right ventricular volume (**b**)

Two methods were used to measure RV volumes, function and mass (see Fig. 1). Method 1 excluded papillary muscle and trabeculae from the RV blood volume by using semi-automatic threshold-based segmentation software. Method 2 included these structures in the endocardial contour and therefore the blood volume. The semi-automatic threshold-based segmentation software was based on the signal intensity distribution of MR images. The voxels within the epicardial contour were classified as either blood or muscle according to their signal intensity, taking into account spatial variations in signal intensity. Based on their signal intensity, trabeculae and pappilary muscles were included in the myocardial volume. Users had the possibility to manually change the threshold level of signal intensities above which voxels are depicted as blood for every slice. Selecting and deselecting individual voxels was possible, for example in case of artefacts due to mechanical pulmonary valve prosthesis. As the semi-automatic threshold-based segmentation software was an integral part of QMass, both methods used the same endocardial and epicardial contours. A more detailed description of the segmentation procedure can be found in Appendix 1.

Stroke volume was defined as end-diastolic volume minus end-systolic volume. Ejection fraction was defined as stroke volume divided by end-diastolic volume. Mass is derived from myocardial volume after multiplying by the density of cardiac muscle, 1.05 g/cm^3. All volumes were indexed for Body Mass Index.

To obtain agreement between observers, 25 randomly selected CMR scans were analysed by a second independent observer. For agreement within one observer, the same 25 scans were analysed a second time by the first observer with an interval of at least 2 weeks between the first and second analysis.

Statistical analyses

The Statistical Package for the social sciences version 16.0 (SPSS Inc, Chicago, IL) was used for all statistical analyses. All statistical tests are two-sided and a p value of less than 0.05 was considered statistically significant.

Descriptive statistics were calculated as mean and standard deviation for normally distributed continuous variables, median with interquartile range (IQR) for non-normally distributed continuous variables and absolute numbers and percentages for dichotomous variables. The manual and semi-automatic methods were compared in terms of RV volume, mass and function by using the paired-samples Student's t test.

The intraobserver agreement coefficient (AC_{intra}) between paired observations was calculated for both observers:

$$AC_{intra} = 100 \cdot (1 - \frac{2 \cdot |Obs_1 - Obs_2|}{Obs_1 + Obs_2}) \qquad (1)$$

For the first observer, the median AC_{intra} was computed. The interobserver agreement coefficient AC_{inter} was also determined. For both observers, the average of the two paired observations was used. The difference in median AC between the manual and semi-automatic method was assessed with a paired Wilcoxon signed rank test.

Linear regression was used to examine the relationship between RV volume measurements when including and excluding trabeculae and papillary muscles.

Results

RV volumes and function

Exclusion (Method 1) instead of inclusion (Method 2) of trabeculae and papillary muscle in the RV blood volume resulted in a significant change in measured RV volumes and function. When Method 1 was compared to Method 2, end-diastolic volumes were 15 ± 4 % (from 140 ± 35 to 120 ± 32 ml/m^2), end-systolic volumes 21 ± 5 % (from 74 ± 23 to 59 ± 20 ml/m^2) and stroke volumes 9 ± 5 %

(from 66 ± 16 to 60 ± 16 ml/m²) smaller ($p < .01$). Ejection fractions were relatively 7 ± 4 % (from 48 ± 7 to 51 ± 8 %) and the end-diastolic masses were 79 ± 21 % (from 28 ± 7 to 51 ± 10 g/m²) larger ($p < .01$). The difference in RV end-diastolic volumes, RV end-systolic volumes, RV ejection fraction and RV end-diastolic mass between method 1 and method 2 increased as volumes, ejection fraction and mass became larger (see Fig. 2).

Exclusion of trabeculae and papillary muscle took an average of 67 ± 16 s extra time compared to inclusion of these structures.

Observer agreement

The intra- and interobserver reproducibility data are shown in Table 2. Observer agreement was high in all measurements with exception of RV mass. Method 1 resulted in a significantly higher AC_{intra} and AC_{inter} for RV mass ($p < .01$). The AC_{intra} for RV end-diastolic volume was significantly higher for Method 2 ($p = .02$).

Model

The amount of trabeculae increased with increasing end-diastolic and end-systolic volumes. Based on this relationship the following model was created:

$$RV_{excl} = a \times RV_{incl} + b \qquad (2)$$

RV_{excl} and RV_{incl} were RV volumes in which the trabeculae and papillary muscles were excluded and included, respectively. For end-diastolic volumes the constant a, b from Eq. 2 were .90 (95 % CI 0.87 to 0.94) and −7.04 ml/m² (95 % CI −2.29 to −11.79 ml/m²), respectively. For end-systolic volumes, a was 0.87 (95 % CI 0.84 to 0.90) and b −5.30 ml/m² (95 % CI −2.64 to −7.96 ml/m²).

Fig. 2 Bland-Altman plots visualizing the differences between method 1 and method 2 for measurements of (a) right ventricular end-diastolic volume, (b) right ventricular end-systolic volume, (c) right ventricular stroke volume, (d) right ventricular ejection fraction and (e) right ventricular end-diastolic mass. The X-axis depicts the mean value of method 1 and method 2 for each parameter. The Y-axis depicts the difference in measurements between method 1 and method 2. The continuous line represents the mean difference between method 1 and method 2 for each measurement and the dotted line represents the mean difference ±1.96 standard deviations between method 1 and method 2. RVED mass = right ventricular end-diastolic mass, RVEDV = right ventricular end-diastolic volume, RVEF = right ventricular ejection fraction, RVESV = right ventricular end-systolic volume, RVSV = right ventricular stroke volume
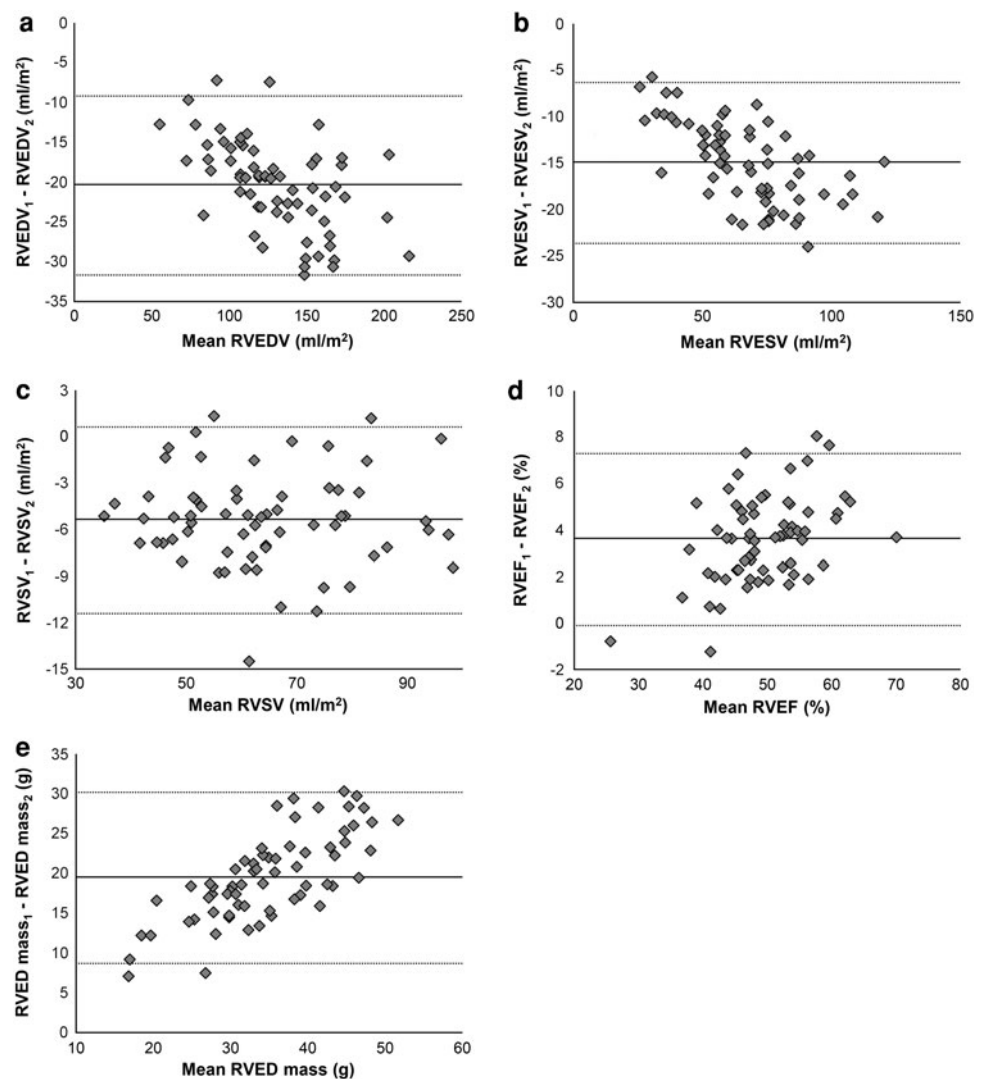
Table 2 Interobserver and intraobserver coefficients of agreement of right ventricular volume and function measurements for method 1 and method 2

	Interobserver						Intraobserver					
	RVEDV	RVESV	RVSV	RVEF	RV mass		RVEDV	RVESV	RVSV	RVEF	RV mass	
Method 1												
Mean diff. ± SD	0.4 ± 7.7	−0.5 ± 6.5	0.6 ± 3.8	0.4 ± 3.9	−2.2 ± 8.8		5.1 ± 6.8	4.2 ± 5.4	0.4 ± 3.4	−1.2 ± 3.6	1.9 ± 4.4	
Limits of agreement	−14.7 to 15.5	−13.3 to 12.2	−6.9 to 8.1	−7.2 to 8.0	−19.4 to 15.0		−8.3 to 18.5	−6.4 to 14.9	−6.3 to 7.2	−8.3 to 5.8	−6.8 to 10.6	
AC (%)	96	95	93	95	87		95	95	95	97	93	
Method 2												
Mean diff. ± SD	1.1 ± 10.7	2.4 ± 7.3	−0.6 ± 4.5	−1.5 ± 3.8	−2.8 ± 7.0		2.7 ± 7.1	3.9 ± 7.2	−0.7 ± 3.3	−1.8 ± 3.6	4.6 ± 3.3	
Limits of agreement	−19.9 to 22.2	−11.9 to 16.6	−9.5 to 8.3	−9.0 to 6.0	−16.5 to 11.0		−11.2 to 16.6	−10.0 to 18.0	−7.1 to 5.7	−8.8 to 5.2	−1.9 to 11.1	
AC (%)	95	94	91	95	78		97	96	93	96	85	
p value	.43	.86	.21	.56	<.01		.02	.19	.72	.40	<.01	

Volumetric data are expressed in ml/m², and mass in g/m². *AC* agreement coefficient, *Method 1* exclusion of papillary muscle and trabeculae in the RV blood volume, *Method 2* inclusion of papillary muscle and trabeculae from the RV blood volume, *RVEDV* right ventricular end-diastolic mass, *RV mass* right ventricular end-diastolic mass, *RVEF* right ventricular ejection fraction, *RVESV* right ventricular end-systolic volume, *RVSV* right ventricular stroke volume

Discussion

Our study is the first to show the impact of trabeculae and papillary muscle on RV volume measurements in a large group of patients with repaired tetralogy of Fallot. Semi-automatic threshold-based segmentation software provided a reproducible method to differentiate myocardium from blood. Compared to including papillary muscle and trabeculae in the RV blood volume, exclusion of the papillary muscle and trabeculae from the RV blood volume resulted in significantly decreased end-systolic and end-diastolic volumes and increased ejection fraction and mass.

Manually delineating RV trabeculae and papillary muscles has a low reproducibility in patients with increased trabeculae and is time-consuming [10]. Therefore, many studies in patients with ToF have included these structures in the blood volume. Our study showed that with semi-automatic threshold-based segmentation software it is possible to differentiate myocardium from blood with a high reproducibility, which is in line with a previous report [11]. This creates the possibility to measure RV blood volume without inclusion of trabeculae and papillary muscles. Inclusion or exclusion of trabeculae and papillary muscles can have a profound effect on the measured volumes and mass. Our study showed a decrease of 21 % in end-systolic volume and 15 % in end-diastolic volume when these structures were excluded from the RV blood pool. The change in measured RV mass was very large with an increase of 79 %.

Most patients with repaired ToF are considered to mainly have a volume-overloaded. We expected the trabeculae to blood volume ratio to be much less in our patients with ToF than reported in patients with systemic RVs. However, compared to patients with systemic RVs in a study by Winter et al., the change in volume was similar in patients with repaired ToF for end-diastolic volume (15 % for both groups) and smaller for the end-systolic volume (21 vs. 27 %) when trabeculae and papillary muscle were excluded from the RV blood pool [10]. It is difficult to compare our results with those from the study by Winter et al. as they delineated trabeculae and papillary muscles manually to differentiate blood from muscle, instead of semi-automatic with threshold-based segmentation software. In our study, no direct comparison was made between these two methods because of the aforementioned disadvantages of manually delineating trabeculae and papillary muscles [10].

Although the amount of trabeculae and papillary muscles should be the same in end-systole and end-diastole, stroke volume was 6 ml/m² larger when including compared to excluding these structures. A possible explanation is that the amount of trabeculae in end-systole was underestimated. Discriminating trabeculae from RV wall is

difficult in end-systole due to compression of the trabeculae against the RV wall. Therefore, contour tracing was aided by reviewing the multiple phase scans in the movie mode. Based on movement and position of the trabeculae during the entire heart cycle, it was possible to interpolate the position of the endocardial contour. Some of the trabeculae were possibly considered to be RV wall in end-systole and not in end-diastole. Another explanation is that the amount of trabeculae was overestimated in end-diastole. Trabeculae can be better distinguished from the RV wall in end-diastole. However, this will result in more voxels containing both blood and trabeculae and too much of these voxels were possibly considered to be trabuculae and not blood.

The existing RV reference values are based on RV volumes including trabeculae and papillary muscles. When papillary muscles and trabeculae are excluded from the blood volume, use of these reference values is no longer valid. Until new reference values are developed in which the trabeculae and papillary muscles are excluded, it is possible to use the proposed model in patients with ToF to allow comparison with the old reference values. The same applies to the application of threshold values. An important threshold is the use of RV end-diastolic volume for timing pulmonary valve replacement in patients with ToF [1–5]. The reported thresholds range from 82–90 ml/m^2 for end-systolic volume and 150–170 ml/m^2 for end-diastolic volumes. Some of these differences may be explained by including or excluding trabeculae and papillary muscles in the measured volumes. Unfortunately, only one of these studies reported whether they included RV trabeculae and papillary muscles in the measured volumes [2].

Limitations and future perspectives

A gold standard for the amount of endocardial trabeculae of the RV is lacking. Therefore, a validation in vivo was not possible. However, exclusion of trabeculae and papillary muscle should be theoretically more accurate as these structures are part of the myocardium and not blood.

In our study, measurements of RV volumes and function were highly reproducibility. However, an axial orientation could have resulted in an even higher reproducibility and also a higher accuracy in patients with a severely dilated RV [16, 17].

Our study was limited to patients with repaired ToF as this is the most common severe congenital heart disease in adult patients. To determine the influence of trabeculae in the RV volume in other patient groups, more research is required. Our study showed that semi-automatic threshold-based segmentation software is a valuable tool for further research in this area.

Conclusion

RV endocardial trabeculae significantly influence measured RV volumes and mass. Exclusion compared to inclusion of trabeculae and papillary muscle in the RV blood volume results in a significantly decrease in measured end-systolic and end-diastolic volume and increase in measured ejection fraction and mass. Semi-automatic threshold-based segmentation software can exclude trabeculae and papillary muscles from the RV blood volume in a reproducible manner. Currently used ranges and thresholds for congenital heart disease patients should be re-established, as new threshold-based algorithms will become available in clinical practice.

Appendix 1

The technique of normalized convolution is used to estimate the spatially varying blood and muscle intensities within a user-provided epicardial contour. The voxel intensity is defined by a first order model with six variables:

$$I(x, y) = (1 - w(x, y)) \times I_m(x, y) + w(x, y) \times I_b(x, y) \quad (3)$$

with:

$$\begin{aligned} Muscle : I_m(x, y) = a_0 + a_1 x + a_2 y \\ Blood : I_b(x, y) = b_0 + b_1 x + b_2 y \end{aligned} \quad (4)$$

where a_0, a_1, a_2, b_0, b_1 and b_2 are constants that vary among scans according to the grey value distribution of the image within the epicardial contour. $I_m(x,y)$ and $I_b(x,y)$ represent the approximation of the intensity of muscle and blood, respectively, at the position (x,y) The constants are obtained with an iterative optimization procedure, during which the weight $w(x,y)$ is initialized to either 1 or 0 using the Otsu threshold method.

The procedure is stopped when the classification $w > 0.5$ is unaltered between iterations or when the number of iterations exceeds ten.

Assuming a linear relationship between the fraction of blood and the intensity of the voxel ($I(x,y)$), the weight $w(x,y)$ represents the fraction of blood in the voxel.

$$w(x,y) = \frac{I(x,y) - I_m(x,y)}{I_b(x,y) - I_m(x,y)} \quad (5)$$

A binary classification is obtained by thresholding $w(x,y)$. If $w(x,y)$ is higher than the threshold value, the voxel is considered pure blood, otherwise it is defined as pure muscle. In this experiment the threshold value was set to 70 %. Blood volume measures are obtained by multiplying the number of voxels classified as blood with the voxel volume.

References

1. Therrien J, Provost Y, Merchant N, Williams W, Colman J, Webb G (2005) Optimal timing for pulmonary valve replacement in adults after tetralogy of Fallot repair. Am J Cardiol 95:779–782

2. Buechel ER, Dave HH, Kellenberger CJ, Dodge-Khatami A, Pretre R, Berger F, Bauersfeld U (2005) Remodelling of the right ventricle after early pulmonary valve replacement in children with repaired tetralogy of Fallot: assessment by cardiovascular magnetic resonance. Eur Heart J 26:2721–2727

3. Oosterhof T, van Straten A, Vliegen HW, Meijboom FJ, van Dijk AP, Spijkerboer AM, Bouma BJ, Zwinderman AH, Hazekamp MG, de Roos A, Mulder BJ (2007) Preoperative thresholds for pulmonary valve replacement in patients with corrected tetralogy of Fallot using cardiovascular magnetic resonance. Circulation 116:545–551

4. Frigiola A, Tsang V, Bull C, Coats L, Khambadkone S, Derrick G, Mist B, Walker F, van Doorn C, Bonhoeffer P, Taylor AM (2008) Biventricular response after pulmonary valve replacement for right ventricular outflow tract dysfunction: is age a predictor of outcome? Circulation 118:S182–S190

5. Geva T (2011) Repaired tetralogy of Fallot: the roles of cardiovascular magnetic resonance in evaluating pathophysiology and for pulmonary valve replacement decision support. J Cardiovasc Magn Reson 13:9

6. Baumgartner H, Bonhoeffer P, De Groot NM, de Haan F, Deanfield JE, Galie N, Gatzoulis MA, Gohlke-Baerwolf C, Kaemmerer H, Kilner P, Meijboom F, Mulder BJ, Oechslin E, Oliver JM, Serraf A, Szatmari A, Thaulow E, Vouhe PR, Walma E, Vahanian A, Auricchio A, Bax J, Ceconi C, Dean V, Filippatos G, Funck-Brentano C, Hobbs R, Kearney P, McDonagh T, Popescu BA, Reiner Z, Sechtem U, Sirnes PA, Tendera M, Vardas P, Widimsky P, McDonagh T, Swan L, Andreotti F, Beghetti M, Borggrefe M, Bozio A, Brecker S, Budts W, Hess J, Hirsch R, Jondeau G, Kokkonen J, Kozelj M, Kucukoglu S, Laan M, Lionis C, Metreveli I, Moons P, Pieper PG, Pilossoff V, Popelova J, Price S, Roos-Hesselink J, Uva MS, Tornos P, Trindade PT, Ukkonen H, Walker H, Webb GD, Westby J, Task Force on the Management of Grown-up Congenital Heart Disease of the European Society of Cardiology (ESC) (2010) ESC Guidelines for the management of grown-up congenital heart disease (new version 2010). Eur Heart J 31:2915–2957

7. Warnes CA, Williams RG, Bashore TM, Child JS, Connolly HM, Dearani JA, del Nido P, Fasules JW, Graham TP Jr, Hijazi ZM, Hunt SA, King ME, Landzberg MJ, Miner PD, Radford MJ, Walsh EP, Webb GD (2008) ACC/AHA 2008 Guidelines for the Management of Adults with Congenital Heart Disease: a report of the American College of Cardiology/American Heart Association Task Force on Practice Guidelines (writing committee to develop guidelines on the management of adults with congenital heart disease). Circulation 118:e714–e833

8. Kilner PJ, Geva T, Kaemmerer H, Trindade PT, Schwitter J, Webb GD (2010) Recommendations for cardiovascular magnetic resonance in adults with congenital heart disease from the respective working groups of the European Society of Cardiology. Eur Heart J 31:794–805

9. Sievers B, Kirchberg S, Bakan A, Franken U, Trappe HJ (2004) Impact of papillary muscles in ventricular volume and ejection fraction assessment by cardiovascular magnetic resonance. J Cardiovasc Magn Reson 6:9–16

10. Winter MM, Bernink FJ, Groenink M, Bouma BJ, van Dijk AP, Helbing WA, Tijssen JG, Mulder BJ (2008) Evaluating the systemic right ventricle by CMR: the importance of consistent and reproducible delineation of the cavity. J Cardiovasc Magn Reson 10:40

11. Beerbaum P, Barth P, Kropf S, Sarikouch S, Kelter-Kloepping A, Franke D, Gutberlet M, Kuehne T (2009) Cardiac function by MRI in congenital heart disease: impact of consensus training on interinstitutional variance. J Magn Reson Imaging 30:956–966

12. Mooij CF, de Wit CJ, Graham DA, Powell AJ, Geva T (2008) Reproducibility of MRI measurements of right ventricular size and function in patients with normal and dilated ventricles. J Magn Reson Imaging 28:67–73

13. Samyn MM, Powell AJ, Garg R, Sena L, Geva T (2007) Range of ventricular dimensions and function by steady-state free precession cine MRI in repaired tetralogy of Fallot: right ventricular outflow tract patch vs. conduit repair. J Magn Reson Imaging 26:934–940

14. Davlouros PA, Kilner PJ, Hornung TS, Li W, Francis JM, Moon JC, Smith GC, Tat T, Pennell DJ, Gatzoulis MA (2002) Right ventricular function in adults with repaired tetralogy of Fallot assessed with cardiovascular magnetic resonance imaging: detrimental role of right ventricular outflow aneurysms or akinesia and adverse right-to-left ventricular interaction. J Am Coll Cardiol 40:2044–2052

15. Alfakih K, Plein S, Thiele H, Jones T, Ridgway JP, Sivananthan MU (2003) Normal human left and right ventricular dimensions for MRI as assessed by turbo gradient echo and steady-state free precession imaging sequences. J Magn Reson Imaging 17:323–329

16. Clarke CJ, Gurka MJ, Norton PT, Kramer CM, Hoyer AW (2012) Assessment of the accuracy and reproducibility of RV volume measurements by CMR in congenital heart disease. JACC Cardiovasc Imaging 5:28–37

17. Fratz S, Schuhbaeck A, Buchner C, Busch R, Meierhofer C, Martinoff S, Hess J, Stern H (2009) Comparison of accuracy of axial slices versus short-axis slices for measuring ventricular volumes by cardiac magnetic resonance in patients with corrected tetralogy of Fallot. Am J Cardiol 103:1764–1769